

1 **Pioreactors at Sea: Assessing Microbial Community Response to**  
2 **Added Dissolved Inorganic Nutrients**

3 Jackson Page-Roth

4 University of Washington, Seattle, WA

5 School of Oceanography

6 02/02/2024

7 [jrproth@uw.edu](mailto:jrproth@uw.edu)

8

## 9 **Abstract**

10 This study aims to understand interactions within the microbial community of the oligotrophic  
11 (nutrient-poor) equatorial Pacific. This experiment attempts to provide a more realistic  
12 representation of in-situ conditions, overcoming previous difficulties capturing the dynamic  
13 behavior of microbial communities in the field. A novel methodology utilizing a continuous  
14 media supply to incubate natural microbial communities from the field accomplishes this  
15 objective. Three growth chambers were employed, one as a continuous incubation control (no  
16 nutrients added), one as a continuous incubation with added inorganic nutrients (nitrate,  
17 phosphate, and silicate), and one as a batch incubation with the same added nutrients. A  
18 continuous incubation constantly exchanges a small volume of external media from outside the  
19 growth chamber with volume from inside the growth chamber. A batch incubation does not have  
20 any media exchanged during its incubation period. All incubations followed a 16:8 light/dark  
21 period using LEDs, simulating environmental day-night cycles. Community response was  
22 assessed by monitoring the turbidity of the incubation with continuous optical density  
23 measurements, with beginning and endpoint subsamples analyzed for total bacterial abundance  
24 and DNA content using flow cytometry. There was a distinct day-night turbidity oscillation in all  
25 incubations, with the nutrient-enriched continuous incubation being the most pronounced  
26 (average normalized optical density 10% greater during simulated daytime). At the conclusion of  
27 the experiment, the continuous incubation without added nutrients had about double the bacterial  
28 cell concentration and a greater bacterial DNA content, yet similar optical density values  
29 compared to its nutrient-added counterpart. This combination of results suggests that the added  
30 nutrients selected for larger, slower growing bacteria, such as the picophytoplankton  
31 *Synechococcus*, which would align with previous studies. Additionally, the different turbidity

32 oscillations between incubation methods suggest that nutrient replenishment results in a greater  
33 microbial response to diel variability. This study not only advances our understanding of  
34 microbial community dynamics in the oligotrophic equatorial Pacific but also introduces a novel  
35 experimental method that can be applied across a diversity of marine and aquatic environments.

## 36 **Plain Language Summary**

37 This study investigated the interactions among microorganisms in the nutrient-poor equatorial  
38 Pacific Ocean. To better simulate conditions these microbes experience in nature, a new  
39 experimental approach was used, involving a continuous media supply to simulate ocean mixing.  
40 All incubations mimicked day and night cycles with built-in LEDs. Community responses were  
41 measured by continuously monitoring optical density, a proxy for microbial biomass, and  
42 beginning and endpoint samples that were analyzed for bacteria cell concentration and size  
43 (estimated by DNA content). Three incubations were used, one as a continuous incubation (no  
44 added nutrients), one as continuous incubation with added inorganic nutrients, and one as a batch  
45 incubation with added inorganic nutrients. The results showed distinct day-night optical density  
46 oscillations in all incubations, with the nutrient-enriched continuous system having the most  
47 significant variation. This implies that the nutrient replenishment from simulated mixing allows  
48 for a greater microbial response to day-night cycles. Bacterial abundance varied across all  
49 systems, indicating different responses from the bacteria in each incubation. This study not only  
50 enhances our understanding of microbial communities in the nutrient-poor equatorial Pacific but  
51 also introduces a new experimental method applicable to various marine and aquatic  
52 environments.

## 53 **1 Introduction**

### 54 1.1 Heterotrophic bacteria and phytoplankton

55 Heterotrophic bacteria serve as integral components of the marine ecosystem and the movement  
56 of nutrients across biota within the ocean. By consuming dissolved organic carbon generated by  
57 marine autotrophs (Azam et al., 1983; le B. Williams, 1998) and recycling the associated  
58 nutrients, heterotrophs are a key influence in controlling marine nutrient fluxes (Azam et al.,  
59 1994).

60 There is a deep, two-way connection between heterotrophic bacteria and phytoplankton, the  
61 predominant marine autotrophs (Fouilland & Mostajir, 2010). Stimulation of phytoplankton  
62 blooms results in more organic nutrients for heterotrophic bacteria, stimulating their growth in  
63 turn (Gomes et al., 2015). Additionally, phytoplankton rely on heterotrophs to recycle organic  
64 nutrients back into inorganic nutrients. Furthermore, heterotrophic bacteria produce and release  
65 vitamins into the water columns that are required by but not produced by phytoplankton (Bratbak  
66 & Thingstad, 1986).

67 All microorganisms, but especially autotrophs, respond to changes in inorganic nutrients. Three  
68 key dissolved inorganic nutrients (DIN) limit marine autotrophic productivity at the surface:  
69 nitrate, phosphate, and silicate (Mackey et al., 2002). Within the central equatorial Pacific, the  
70 predominant two autotrophs are the picophytoplankton *Prochlorococcus* and *Synechococcus*.  
71 More specifically, within nutrient-depleted surface waters of the equatorial Pacific,  
72 *Synechococcus* is the most dominant, while *Prochlorococcus* is most dominant at depths of 100–  
73 125 meters (Mackey et al., 2002). Both picophytoplankton and heterotrophic bacteria co-exist in  
74 this area at typical cell densities on the order of  $10^5$  cells  $\text{mL}^{-1}$  (Mackey et al., 2002; Lim, 2023).  
75 This concentration is relatively low in the global ocean. For example, the northeast Atlantic  
76 Ocean has typical concentrations of these organisms on the order of  $10^6$  cells  $\text{mL}^{-1}$  (Lim, 2023).

77 1.2 El Niño Southern Oscillation

78 Phytoplankton in equatorial Pacific waters are limited by DIN availability (Mackey et al., 2002).  
79 Therefore, an addition of DIN into the system should result in an increase in biological  
80 productivity. DIN are found in lower concentrations during El Niño (Mackey et al., 2002). El  
81 Niño events occur every few years due to the weakening of equatorial trade winds by decreased  
82 surface warming. This weakening can occur for various reasons, but this process oscillates with  
83 stronger equatorial winds with increased surface warming, known as La Niña (Timmermann et  
84 al., 2018). This cycle is known as the El Niño Southern Oscillation. Due to decreased easterly  
85 trade winds during El Niño, upwelling also decreases across the equatorial Pacific. Decreased  
86 upwelling results in lower nutrient concentrations, specifically nutrients that are found in greater  
87 concentration below the mixed layer (Mackey et al., 2002). This process can result in even  
88 greater oligotrophic conditions at the surface (Ducklow et al., 1996). Oligotrophic environments  
89 are classified by both low nutrient flux and low ambient nutrient concentrations (Schut et al.,  
90 1997). Conversely, during La Niña seasons, upwelling is increased at the equator, increasing  
91 nutrient concentrations that can drive phytoplankton blooms and overall biological productivity  
92 (Ryan et al., 2006). The hypothesis motivating this study is that an increased supply of inorganic  
93 nutrients will stimulate the growth of *Synechococcus*, the larger of the two picophytoplankton in  
94 this region.

### 95 1.3 Comparing microbial culturing methodologies

#### 96 1.3.1 Culturing versus incubation

97 Given the importance of understanding the microbial communities that inhabit the ocean, there  
98 have been countless different culturing and incubation methods utilized over the years to  
99 evaluate their potential behaviors in situ. In this study, use of the term “culture” refers  
100 predominantly to a pure culture grown from an isolated strain and thus to culturing it in the lab.

101 While there are mixed cultures, or cultures containing more than one microbe, used in lab  
102 experiments, these cultures are unable to mimic an entire microbial community from nature.  
103 Therefore, this experiment uses the term “incubations” to refer to the facilitated growth of a  
104 natural microbial community. However, many of the techniques this experiment used to analyze  
105 the community response during an incubation were inspired by pre-existing culturing  
106 methodologies.

### 107 1.3.2 Batch culture

108 A batch culture is one of the simplest methods to grow microbes in a controlled environment. In  
109 a batch culture, a single strain is inoculated into its growth media, such as a bottle of defined,  
110 nutrient-rich media. Growth is then observed over time through various methods (flow  
111 cytometry, microscopy, optical density, etc.) to calculate a growth rate of the organism. Multiple  
112 batches can easily be run in parallel to obtain replicates, test different growth media, test  
113 different microbes, etc. (MacIntyre & Cullen, 2009)

### 114 1.3.3 Fed batch culture

115 A fed batch culture is very similar to a standard batch culture, except that it receives continuous  
116 addition of media. No media is removed from the system, only added. The rate at which media is  
117 supplied controls the nutrient content within the growth chamber, therefore controlling microbial  
118 growth (Minihane & Brown, 1986). However, due to no media being removed, this method  
119 requires a growth chamber large enough to accommodate all the added media, rendering it  
120 difficult to use for long term experiments, or experiments that are small scale. This method is  
121 very common in the culturing of baker’s yeast, where a large final quantity is desirable, and  
122 allows for constant fine tuning of the nutrient content within the growth chamber.

123 1.3.4 Turbidostat culture

124 A turbidostat culture is a semicontinuous culturing method that controls microbial growth by  
125 diluting the growth media. It relies on a sensor to measure the optical density within the growth  
126 chamber and automatically dilute the culture when that turbidity reaches a certain value  
127 (MacIntyre & Cullen, 2009). This technique can estimate growth rate in pure cultures where the  
128 average cell size does not dramatically change throughout the experiment.

129 1.3.5 Chemostat culture

130 Every microbial growth rate is determined by its environment. A chemostat culture is a  
131 continuous culturing method where microbial growth is restricted by the frequency at which  
132 limiting nutrients are added to the system (MacIntyre & Cullen, 2009). Two main factors  
133 influence how quickly microbes can grow in a continuous culture: media exchange rate and  
134 nutrient concentration. These two variables can be scaled together and allow for variable growth  
135 rates in a microbial community. For example, a highly nutrient rich media typically can be in  
136 equilibrium with a culture using a faster exchange rate than a lower nutrient media and will  
137 therefore have a greater microbial growth rate. This method allows for the experimenter set the  
138 nutrient content and exchange rate of the culture. Over a culturing period, the culture may adapt  
139 to its environment, allowing it to grow out of an equilibrium state.

140 1.3.6 Continuous incubation

141 This experiment uses a continuous incubation methodology. As defined here, a continuous  
142 incubation starts with a natural microbial community and all the organisms present in it. There is  
143 no isolation of any culture, pure or mixed, as the goal is to work with a natural community  
144 provided with an environment as close to in-situ as possible. Second, instead of nutrients being

145 added according to the response of the microbial community, as in the turbidostat, media is  
146 added and removed from the growth chamber (like a chemostat) consistently throughout the  
147 entire experiment. Because the incubation includes the natural microbial community, it cannot be  
148 classified as a chemostat due to the microbial interactions constantly occurring never allowing  
149 the incubation to be in equilibrium.

### 150 1.3.7 Scientific need for continuous incubations

151 The environmental variables discussed in Section 1.2 are tightly intertwined with one another,  
152 and understanding how they covary has proven difficult. For example, oligotrophic marine  
153 heterotrophic bacteria have been notoriously difficult to isolate in culture, even when provided  
154 both optimal temperature and nutrient conditions. Research has been conducted on organic  
155 carbon fluxes and mineralization, interactions between marine autotrophs and heterotrophic  
156 bacteria, productivity of heterotrophic bacteria, heterotrophic bacterial concentration with depth,  
157 etc. (Schut et al., 1997; Ducklow & Kirchman, 2000; Lim, 2023). However, no prior experiment  
158 has analyzed the effects of added DIN on a natural microbial community in a continuous  
159 incubation.

160 This study analyzes how the equatorial Pacific microbial community responds to the addition of  
161 nitrate, phosphate, and silicate in different incubation methods. The addition of DIN attempts to  
162 simulate a change in environmental conditions that microbes experience during a shift from El  
163 Niño to La Niña.

### 164 1.4 The Pioreactor system

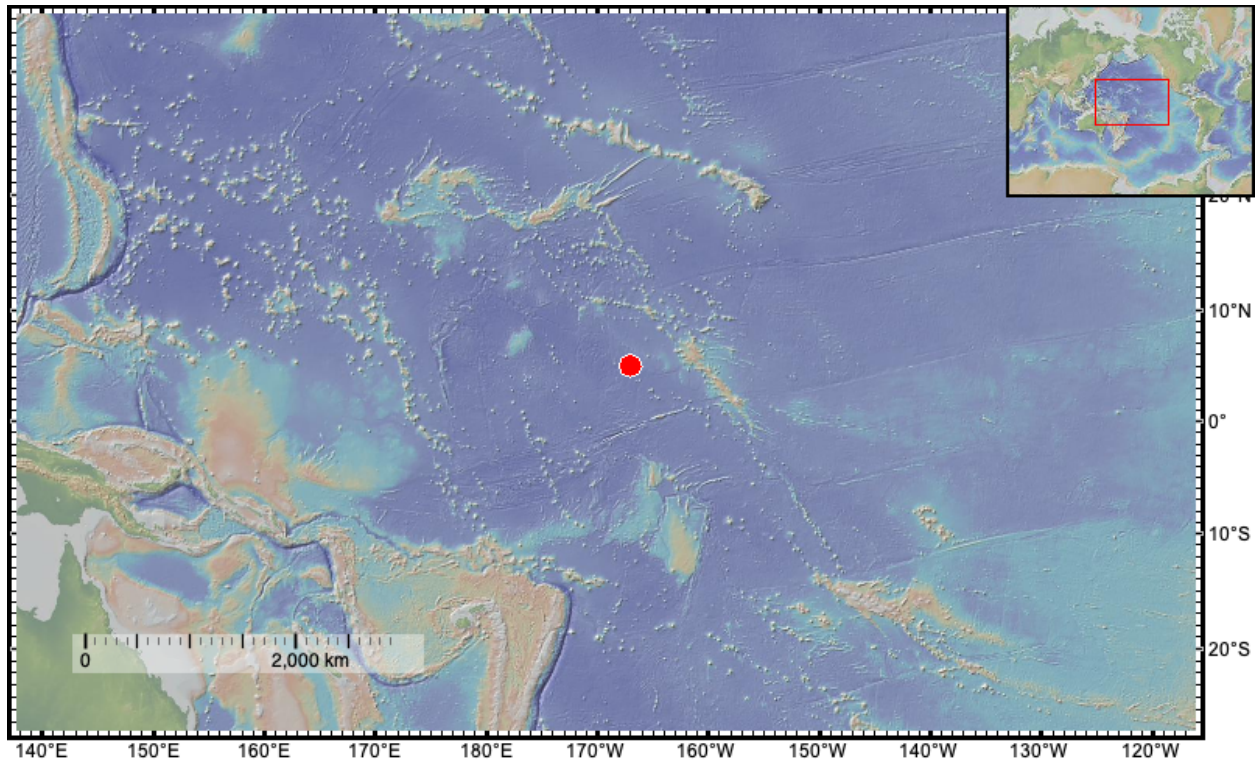
165 This experiment utilized 3 Pioreactors (Pioreactor, Waterloo, ON, Canada) to conduct the  
166 incubations. A Pioreactor is a small, 3D printed bioreactor that is controlled by a custom user

167 interface on a Raspberry Pi. Its small footprint (9 x 15 x 15 cm with pumps) and reasonable price  
168 (~\$250 per unit) make it incredibly useful for field deployments when compared to larger  
169 incubators that could be similarly customized. Features include a built-in and customizable  
170 optical density sensor, controllable mixing with a magnetic stir bar, temperature control, and the  
171 ability to power multiple external loads, such as peristaltic pumps and additional LEDs. The  
172 growth chamber has a working volume of 15 mL, and the complete chamber and tubing system  
173 can be easily autoclaved. During incubation, the system can automatically calculate optical  
174 density normalized to starting density and estimate growth rate. Multiple Pioreactors can be  
175 linked together into a cluster and controlled through one “leader.” The entire system uses Wi-Fi  
176 for communication between units and allows for a browser-based control interface. It also has  
177 the capability for its own local network, allowing for operation without an external Wi-Fi source.  
178 There are some limitations of the system, namely the small growth chamber and occasional  
179 software difficulties. However, when compared to traditional culturing and incubation systems,  
180 the Pioreactor system allows for much greater customizability and control across multiple  
181 variables, with real-time growth measurements.

## 182 **2 Methods**

### 183 2.1 Sampling procedure

184 Samples were collected aboard the R.V. *Thomas G. Thompson* on 6 January 2024, at 5°N,  
185 167°W (Figure 1). The collected samples were collected by 10 L Niskin bottles from a depth of  
186 40 m and transferred into sample-rinsed 1 L Nalgene bottles. Each sample was prefiltered  
187 through a 47 mm, 3 µm filter into a 1 L beaker using a vacuum pump (Figure 2a). This step  
188 aimed to eliminate large grazers and other organisms that could introduce variability among  
189 smaller vial sizes.



190

191 **Figure 1. Location of sampling site.** Sample sight is the red point (5°N, 167°W). Samples were  
192 collected at a depth of 40 m.

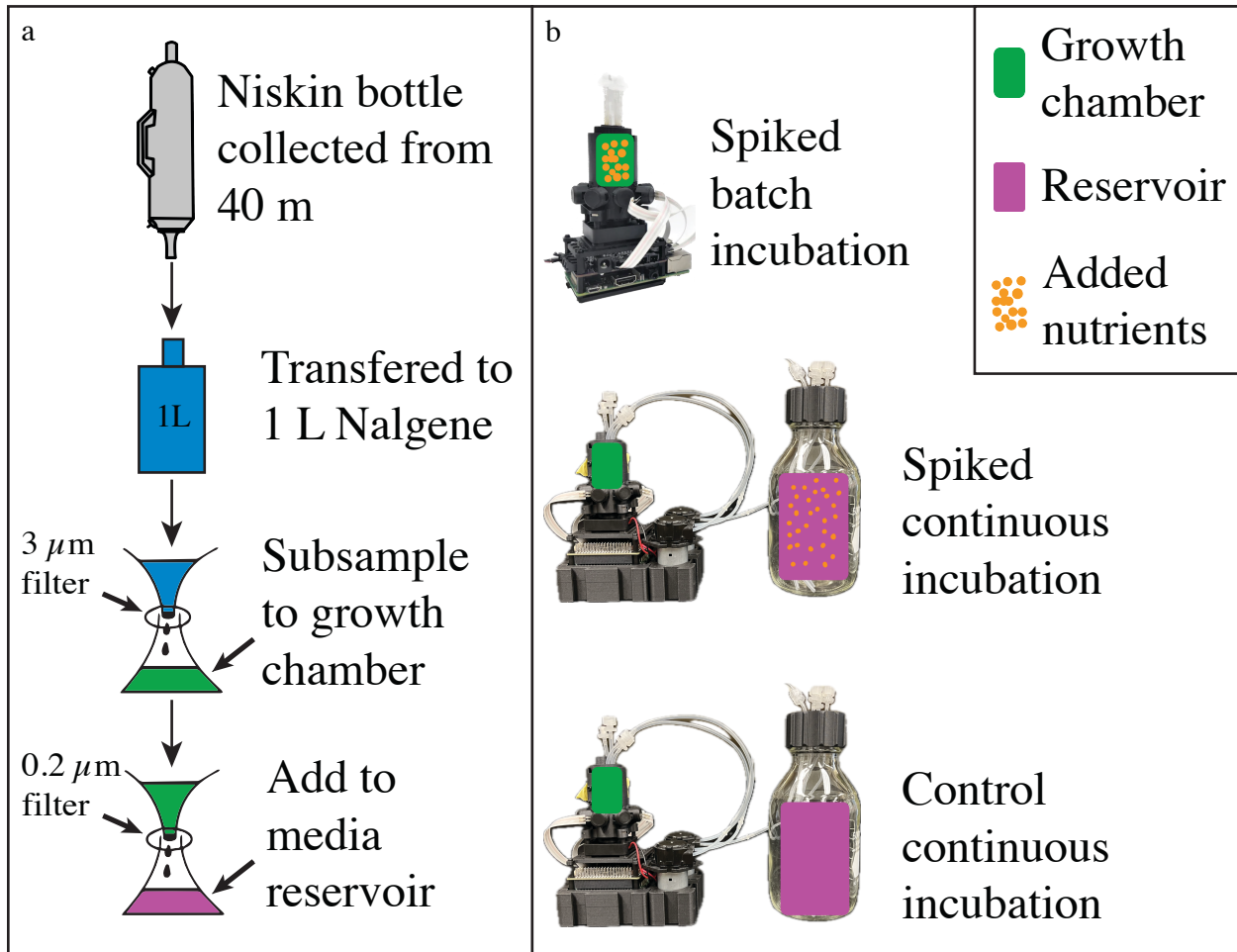
193

## 194 2.2 Media preparation

195 The remaining seawater from the beaker was filtered through a 47 mm, 0.2 µm filter into a 1 L  
196 beaker using a vacuum pump. This filtered seawater served as the reservoir media for the  
197 continuous incubations (Figure 2a).

## 198 2.3 Preparation of Pioreactors

199 Three subsamples of 15 mL from the 3 µm filtered seawater were pipetted into the three  
200 Pioreactor growth chambers (Figure 2b).



201

202 **Figure 2. Diagram of experimental design.** a) Seawater sampling and processing procedure.  
 203 Water was collected from 40 meters before undergoing a 2-step filtration. After the first filtration  
 204 (3  $\mu\text{m}$ ), 15 mL of the filtrate were transferred into each of the three Pioreactor growth chambers.  
 205 After the second filtration (0.2  $\mu\text{m}$ ), this (microbe-free) filtrate was transferred to the continuous  
 206 incubation reservoirs to serve as the media. b) Layout of the incubation setup. The spiked batch  
 207 incubation had no media input, but DIN was added to the 3  $\mu\text{m}$  filtered seawater in the growth  
 208 chamber. The spiked continuous incubation had DIN added to its media reservoir. No DIN was  
 209 added to the control continuous incubation.

210

211 2.4 Nutrient addition

212 Nitrate, phosphate, and silicate were added to the spiked incubations to double the estimated  
213 nutrient content (Table 1). These inorganic nutrients were added to the media reservoir in the  
214 spiked continuous incubation and directly to the growth chamber for the spiked batch system  
215 (Figure 2b). Initial nutrient concentrations were estimated using the SeaState model (Armbrust  
216 Lab) for the day of sampling in the region. Actual concentrations were then updated after the  
217 cruise with measured nutrient content.

218

219 **Table 1. Estimated nutrient concentrations of the ambient seawater.** Ambient values  
220 calculated from nutrient analysis conducted after the cruise. Spiked values were initially  
221 calculated based on assumed ambient concentrations, to which nutrients were added. These  
222 values were then updated using the actual ambient concentrations determined after the cruise.

Nutrient	Estimated ambient concentration ( $\mu\text{M}$ )	Measured ambient concentration ( $\mu\text{M}$ )	Final spiked concentration ( $\mu\text{M}$ )
Silicate	3.70	1.03	4.83
Nitrate	1.50	0.20	1.70
Phosphate	0.52	0.27	0.77

223

224 2.5 Incubations

225 All incubations were exposed to a 16:8-hour day-night cycle using two built-in LEDs set to draw  
226 5 mA when on. These LEDs had peak wavelengths of 505 and 630 nm. Temperature was set to

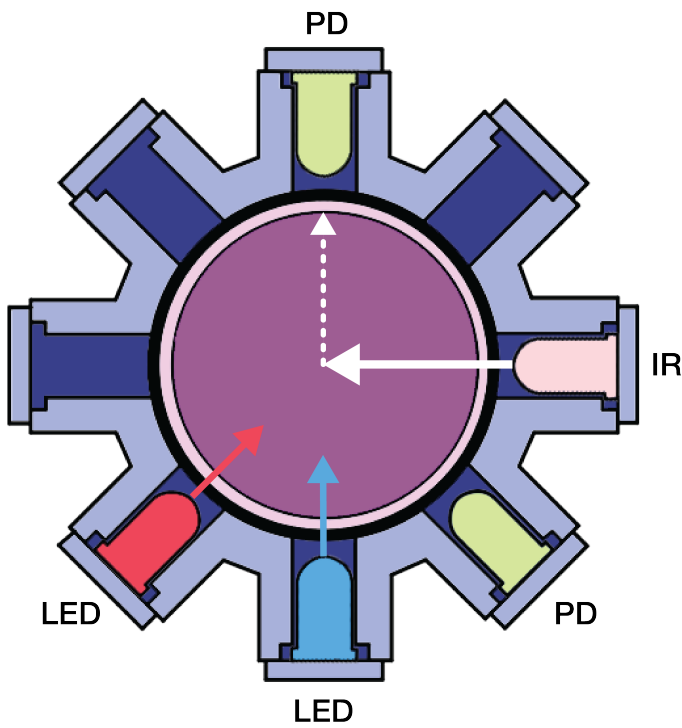
227 30°C using the built-in heating printed circuit board (PCB), and each growth chamber  
228 maintained a stirring rate of 500 rpm using a small (sterile) stir bar. The continuous systems  
229 utilized peristaltic pumps to add reservoir media into the growth chamber at a rate of 9 mL day<sup>-1</sup>  
230 (0.6 day<sup>-1</sup> dilution rate). Volume was removed at the same rate to keep the growth chamber  
231 volume the same. Waste tubing ran from the growth chamber into 100 mL waste bottles (Figure  
232 3).

233 In both types of continuous incubations, media was dispensed manually to fill the tubing  
234 between the media reservoir and the growth chamber. This step resulted in unequal initial dosing  
235 between the continuous incubations. There was an early spike in optical density for both  
236 continuous incubations before they returned to average levels after the first day cycle. To allow  
237 for a more direct comparison across samples, this analysis focuses on all optical density values  
238 measured after the initial 24-hour period. The spiked batch incubation did not have any early  
239 spike in optical density, since there was no manual dosing of media. However, there was no  
240 significant change in optical density trends over the first 24 hours and it followed the same trend  
241 as the rest of the incubation.

## 242 2.6 Optical density

243 During the entire experiment, the optical density of each incubation was measured every 5  
244 seconds with the built-in infrared LED and reference photodiodes (Figure 3). To prevent LED  
245 mixing, the system was set to briefly (about 0.25 seconds) turn off the day-night cycle LEDs  
246 whenever an optical density measurement was taken. The angle of the reference photodiodes can  
247 be changed to resolve different levels of turbidity. In this experiment, the reference photodiode  
248 was set to a 90° angle. This frequency of measuring, along with the very low initial cell counts  
249 (~10<sup>5</sup> cells/mL) present in the water column, resulted in the raw data containing noise.

250 Additionally, each raw optical density measurement was not necessarily directly comparable to  
251 another incubation due to inherent variability in the infrared and reference LEDs. To resolve this  
252 problem, a normalization method was used. For each incubation, the average of the first five  
253 values for optical density (over the first 25 seconds) was assigned the value of 1 as the basis for  
254 normalizing subsequent optical density measurements. The first 5 values were taken to account  
255 for the noise within each optical density reading. To better visualize the optical density trends  
256 within the incubation, a rolling average was taken with a 1-hour window (Figure 4).



257  
258 **Figure 3. Diagram of infrared LED and reference photodiodes measuring optical density.**  
259 The growth chamber schematic is shown in purple; not shown is the mixing bar at its base. The  
260 reference angle of 90° between the infrared (IR) photodiode and reference photodiode (PD) is  
261 shown with white arrows. The two LEDs (LED) used for the day-night cycle are shown in blue  
262 and red (figure adapted from pioreactor.com).

263

264           2.7 End point subsampling and flow cytometry

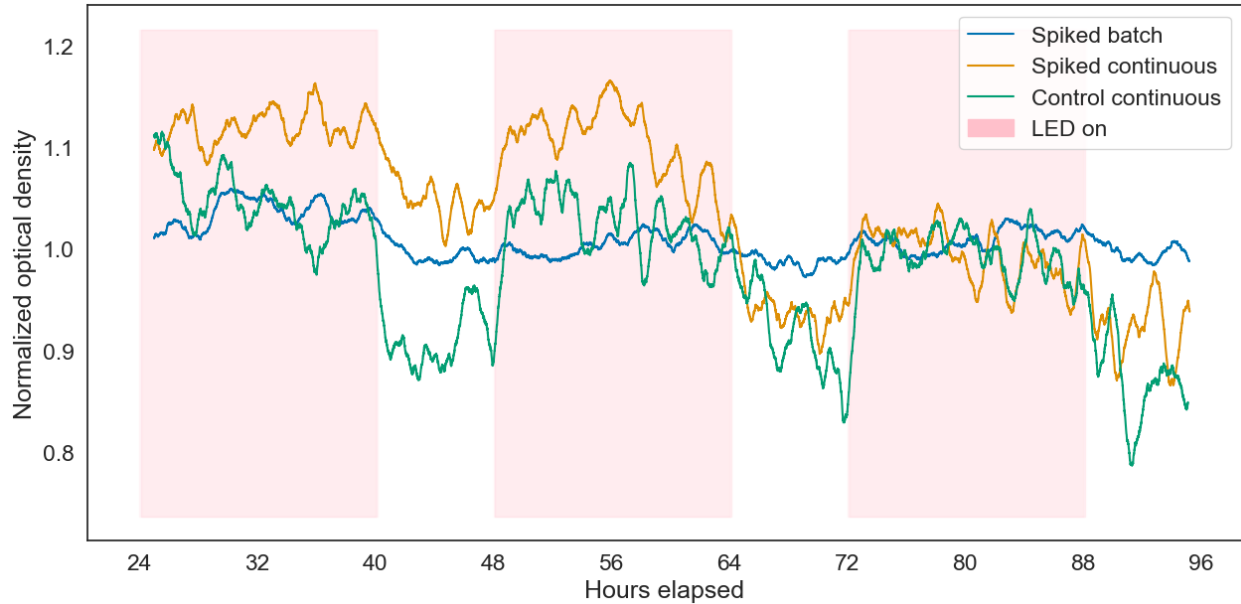
265    At the beginning of the experiment, 4 mL of each 3 µm filtered seawater sample were transferred  
266    to 2 mL cryovials (2 mL per vial) for flow cytometry analysis. This process was repeated at the  
267    end of the experiment, when 4 mL of each Pioreactor growth chamber were pipetted into 2 mL  
268    cryovials (2 mL per vial). All cryovials were immediately stored at –80°C and transported back  
269    to land in a liquid nitrogen storage dewar. At the conclusion of the cruise, samples were stained  
270    with SYBR® Green I and counted on a flow cytometer (Guava easyCyte, Millipore Corporation,  
271    Billerica, MA). This process was conducted by the Morris Lab. Flow cytometry results provided  
272    estimated bacterial cell counts for each sample, as well as DNA content. Fluorescent SYBR®  
273    Green I binds to DNA, allowing for detection of all cells containing DNA within its range of  
274    measurement. DNA content is then calculated by estimating the relative ploidy number, and  
275    therefore DNA content in each cell (Darzynkiewicz et al., 2010).

276

277    **3 Results**

278           3.1 Optical density

279    After normalization and a rolling mean is applied to the optical density measurements (see  
280    section 2.6), three immediate trends are apparent. First, greater optical densities were observed  
281    while the LEDs were on (day-time) than when off (night-time). Second, the continuous  
282    incubations both had greater day-time optical density averages than the batch incubation. Finally,  
283    there was a noticeable decrease in day-time averages during the third day for both continuous  
284    incubations (Figure 4).

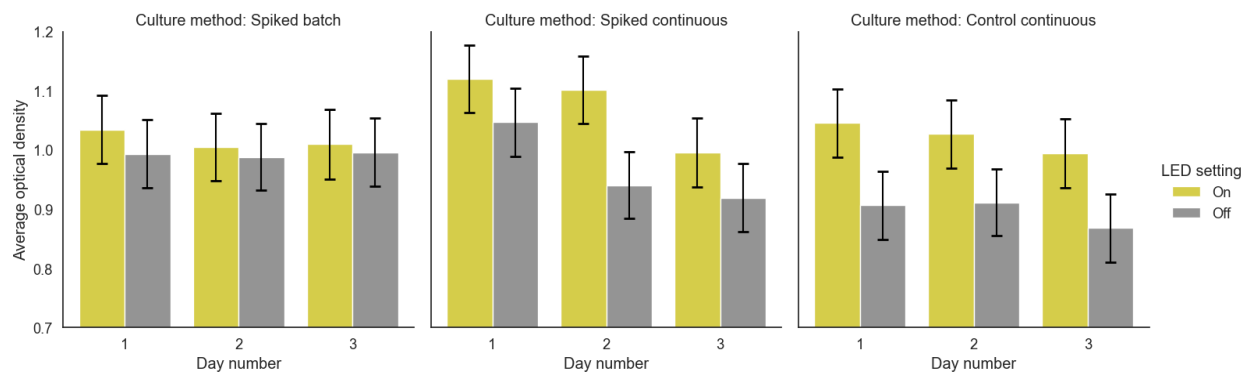


285

286 **Figure 4. Normalized 1-hour-window rolling average of optical density for all three**  
 287 **incubations.** The first 24 hours were omitted (see section 2.5). Pink highlighted sections  
 288 represent the simulated day-time phase. While this figure more clearly displays the trends within  
 289 the data, it is inherently reliant on the initial normalization.

290

291 Within both continuous incubations, a statistically relevant oscillation in optical density was  
 292 observed ( $p$ -value  $< 0.01$  with independent t-test comparing the day and night phases for each  
 293 day). Although less visibly discernible, oscillation also occurred in the spiked batch system ( $p$ -  
 294 value  $< 0.01$  with same test as above). The difference between the average normalized optical  
 295 density values for each incubation during the day and night is as follows: spiked batch, 0.022;  
 296 spiked continuous, 0.097; and control continuous, 0.115. The variability resolved by the optical  
 297 density for continuous incubations is 4–5 times greater than that of the batch incubation (Figure  
 298 5).

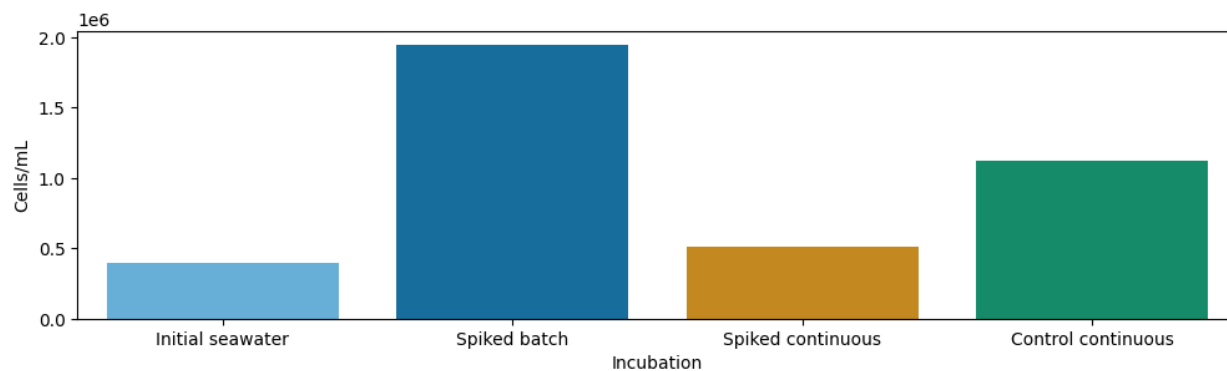


299  
 300 **Figure 5. The average day and night optical densities for each incubation.** Error bars plot the  
 301 standard deviation of the mean for each day (n = 11520) and night (n = 5760) phase.

302

303 **3.2 Cell counts**

304 For all three incubations, the endpoint cell counts were greater than the initial seawater sample  
 305 (Figure 6). Additionally, all three incubations ended with different cell counts. The spiked batch  
 306 incubation ended with the highest cell densities, followed by the control continuous incubation,  
 307 and finally the spiked continuous incubation. Due to an error in the setup of the flow cytometer,  
 308 counts by cell size fractionation were not available for this experiment.



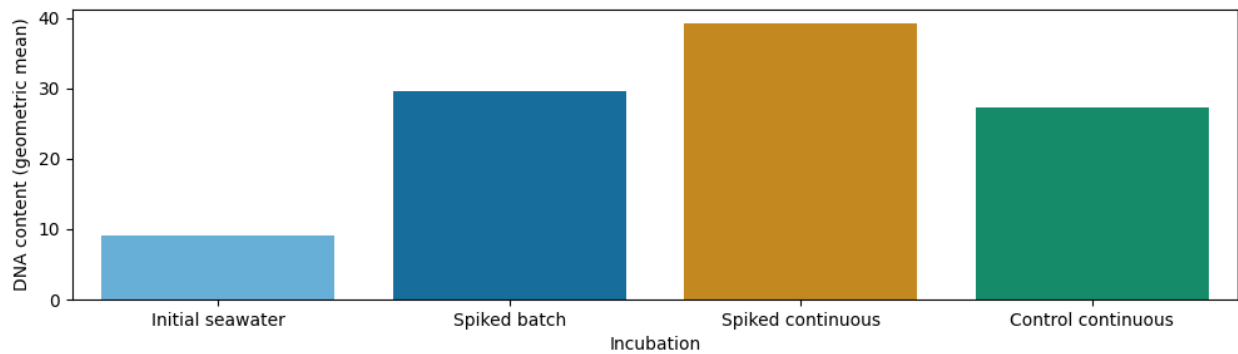
309

310 **Figure 6. Cell counts for initial and endpoint incubation subsamples.** Plotted are the cell  
311 counts (cells/mL) by flow cytometry for the initial 3  $\mu$ m filtered seawater, as well as the endpoint  
312 subsamples for each incubation method.

313

### 314 3.3 DNA content

315 All three endpoint subsamples contained a different DNA content, with the spiked continuous  
316 incubation having a greater DNA content than the control continuous incubation. The initial  
317 seawater DNA content was the lowest of the samples at a relative value of 9.07. The sample with  
318 the greatest DNA content was the spiked continuous incubation with a value of 39.27, while the  
319 control continuous incubation and spiked batch had similar values of 27.29 and 29.64,  
320 respectively (Figure 7).



321

322 **Figure 7. DNA content of incubation subsamples.** Plotted are the DNA contents, measured as  
323 geometric mean by flow cytometry, for the initial 3  $\mu$ m filtered seawater and the endpoint  
324 subsamples for each incubation method.

325

## 326 4 Discussion

#### 327 4.1 Method significance

328 The novel method utilized in this experiment has the potential to allow for a much greater  
329 understanding of microbial community dynamics across a wide range of locations. By utilizing  
330 the same seawater (prefiltered) from which the microbial community originated as the incubation  
331 media, a more accurate representation of in-situ conditions can be achieved. Additionally, the  
332 ability to gather real-time, high-resolution optical density measurements during an incubation,  
333 even with oligotrophic conditions and cell densities on the order of  $10^5 \text{ mL}^{-1}$ , is unprecedented.  
334 While these readings do not necessarily reflect all the changes the microbial community is  
335 undergoing (different microbes of different sizes scatter light differently), they allowed for a  
336 clear picture of overall community trends. Coupling the optical density measurements with  
337 additional instruments, such as a fluorometer, would be a natural next step for this type of  
338 experiment. The ability to control for light, temperature, stirring rate, and media dosing allows  
339 for a highly scalable system for future work across multiple fields of microbiology.

340 These continuous incubation methods represent a departure from traditional batch cultures and  
341 resulted in a different community response. While the approach was hindered by the incubation  
342 size of 15 mL, which restricted subsampling volumes, and the additional setup required to  
343 operate the system, it allowed for a far greater level of control over the variables that affected the  
344 incubation than can be achieved with other methods.

#### 345 4.2 Comparing incubation methodologies

346 A batch incubation methodology yielded a different microbial growth response than a continuous  
347 incubation, both from an optical density and flow cytometry perspective. Continuous incubations  
348 had a very evident day-night oscillation in optical density, a feature that would be difficult to  
349 resolve without a live optical density reading. This result revealed a previously overlooked area

350 of incubation methodologies. Because of the continuously added media, the microbial  
351 community was able to respond to the day-night cycle differently than if no media had been  
352 supplied. Even if a well-controlled batch culture was analyzed consistently across multiple days  
353 with a day-night cycle, this response likely would have been underestimated if not undetected.  
354 All incubations had greater endpoint cell counts than the initial seawater, implying that cell  
355 division had occurred during the incubation period. Each type of incubation ended with a  
356 different density of cells, likely due to the selection of different organisms with different growth  
357 rates. This is further supported by the differing DNA content across the three incubations,  
358 particularly between the spiked and control continuous incubations. The continuous systems had  
359 lower cell counts than the spiked batch. However, they were being diluted over the course of the  
360 experiment, while the spiked batch had no media added or removed.

#### 361 4.3 Nutrient content changes the microbial community

362 For the two continuous incubations, the only difference was the addition of extra nitrate, silicate,  
363 and phosphate. While both incubations resulted in similar optical density curves, their flow  
364 cytometry cell counts and DNA content were quite different. The spiked continuous incubation  
365 ended with about 130% greater bacterial DNA content, but only about 50% of the cell density  
366 compared to the control continuous incubation. The end-point optical density of both incubations  
367 was very similar as well. DNA content can be a proxy for cell size (larger cells tend to have a  
368 higher ploidy, see Darzynkiewicz et al., 2010), which would explain the discrepancy between  
369 cell count and DNA content. Within the spiked continuous incubation, the dominant bacteria  
370 may have been larger in cell size but dividing less frequently than in the control continuous  
371 incubation. This interpretation would also align with my hypothesis that added nutrients would  
372 select for the picophytoplankton *Synechococcus*, which is larger than its common counterpart

373 *Prochlorococcus* (Morel et al., 1993). The other potential reason for the cell size, DNA content,  
374 and optical density discrepancies would be that while optical density captures the turbidity of  
375 everything inside the growth chamber, including live and dead cells, detritus, bubbles, etc., the  
376 flow cytometry measurements focused on bacteria, potentially missing some of the larger  
377 organisms (2–3  $\mu\text{m}$ ) that would have the greatest impact on optical density. In either case, the  
378 added nutrients affected the optical density, bacterial cell counts, and bacterial DNA content of  
379 the incubation, while still retaining the same general response to the day-night cycle as the  
380 control continuous incubation, which most closely resembled in-situ conditions.

## 381 **5 Conclusion**

382 This experiment revealed important differences between incubation methodologies, especially  
383 when attempting to replicate in-situ conditions. Traditional batch culturing (closed system)  
384 allows for the least number of controlled variables and the most distant set of conditions from the  
385 in-situ environment. Even a batch incubation of a microbial community is not a good analogue to  
386 determine in-situ responses to environmental changes, as the removal and replenishment of  
387 nutrients is a key factor in how microbes respond to their environment. While no experiment will  
388 perfectly replicate an in-situ environment, a continuous incubation does an effective job of  
389 simulating mixing. With a small, customizable culturing setup such as the Pioreactor system,  
390 field-based, continuous incubations with real-time optical density values can be achieved.

391 Optical density results display a prominent day-night cycle when the incubation has continuous  
392 media cycling, as opposed to a much lesser response in a batch incubation. Additionally, the  
393 differing final cell counts for each incubation method imply that different methods select for  
394 different microbes. Further studies are needed to determine how closely a continuous incubation  
395 experiment mimics in-situ selection.

396 **Acknowledgements**

397 I would like to thank my advisor for this project, Dr. Francois Ribalet. Additionally, I would like  
398 to thank Dr. Jody Deming and Georges Kanaan for their continued mentorship and advice, as  
399 well as the rest of the UW Oceanography senior thesis professors. I would like to give a big  
400 thank you to Cameron Davidson-Pilon, whose responsiveness to troubleshooting the Pioreactor  
401 system was invaluable. I would also like to thank the captain and crew of the R.V. *Thomas G.*  
402 *Thompson* for allowing this research to be possible. Finally, I would like to thank all my  
403 classmates and peers who supported and advised me on this project.

404 **References**

405 Azam, F., Fenchel, T., Field, J. G., Gray, J. S., Meyer-Reil, L. A., & Thingstad, F. (1983). The  
406 Ecological Role of Water-Column Microbes in the Sea. *Marine Ecology Progress Series*, 10(3),  
407 257–263.

408 Azam, F., Smith, D. C., Steward, G. F., & Hagström, Å. (1994). Bacteria-organic matter  
409 coupling and its significance for oceanic carbon cycling. *Microbial Ecology*, 28(2), 167–179.  
410 <https://doi.org/10.1007/BF00166806>

411 Bratbak, G., & Thingstad, T. F. (1986). Phytoplankton-bacteria interactions: An apparent  
412 paradox? Analysis of a model system with both competition and commensalism. *Deep Sea*  
413 *Research Part B. Oceanographic Literature Review*, 33(3), 236. [https://doi.org/10.1016/0198-](https://doi.org/10.1016/0198-0254(86)91170-2)  
414 [0254\(86\)91170-2](https://doi.org/10.1016/0198-0254(86)91170-2)

415 Darzynkiewicz, Z., Halicka, H. D., & Zhao, H. (2010). Analysis of Cellular DNA Content by  
416 Flow and Laser Scanning Cytometry. *Advances in Experimental Medicine and Biology*, 676,  
417 137–147.

418 Ducklow, H., & Kirchman, D. (2000). Bacterial Production and Biomass in the Oceans. In  
419 *Microbial Ecology of the Oceans*.

420 Ducklow, H. W., Quinby, H. L., & Carlson, C. A. (1996). Bacterioplankton dynamics in the  
421 equatorial Pacific during the 1992 El Nino. *Oceanographic Literature Review*, 2(43), 172.

422 Fouilland, E., & Mostajir, B. (2010). Revisited phytoplanktonic carbon dependency of  
423 heterotrophic bacteria in freshwaters, transitional, coastal and oceanic waters: Phytoplanktonic  
424 carbon dependency of heterotrophic bacteria. *FEMS Microbiology Ecology*, 73(3), 419–429.  
425 <https://doi.org/10.1111/j.1574-6941.2010.00896.x>

426 Gomes, A., Gasol, J. M., Estrada, M., Franco-Vidal, L., Díaz-Pérez, L., Ferrera, I., & Morán, X.  
427 A. G. (2015). Heterotrophic bacterial responses to the winter–spring phytoplankton bloom in  
428 open waters of the NW Mediterranean. *Deep Sea Research Part I: Oceanographic Research*  
429 *Papers*, 96, 59–68. <https://doi.org/10.1016/j.dsr.2014.11.007>

430 Lim, E. (2023). *Changes in bacterial concentrations with depth, temperature, and chlorophyll*  
431 *fluorescence in the Equatorial Pacific Ocean*.  
432 <https://digital.lib.washington.edu:443/researchworks/handle/1773/50946>

433 MacIntyre, H. L., & Cullen, J. J. (2009). Using cultures to investigate the physiological ecology  
434 of microalgae. In R. A. Andersen, *Algal culturing techniques* (Nachdr., pp. 287–326). Elsevier  
435 Academic Press.

436 Mackey, D. J., Blanchot, J., Higgins, H. W., & Neveux, J. (2002). Phytoplankton abundances  
437 and community structure in the equatorial Pacific. *Deep Sea Research Part II: Topical Studies in*  
438 *Oceanography*, 49(13), 2561–2582. [https://doi.org/10.1016/S0967-0645\(02\)00048-6](https://doi.org/10.1016/S0967-0645(02)00048-6)

439 Minihane, B. J., & Brown, D. E. (1986). Fed-batch culture technology. *Biotechnology Advances*,  
440 4(2), 207–218. [https://doi.org/10.1016/0734-9750\(86\)90309-5](https://doi.org/10.1016/0734-9750(86)90309-5)

441 Morel, A., Ahn, Y.-H., Partensky, F., Vaultot, D., & Claustre, H. (1993). Prochlorococcus and  
442 Synechococcus: A comparative study of their optical properties in relation to their size and  
443 pigmentation. *Journal of Marine Research*, 51(3), 617–649.  
444 <https://doi.org/10.1357/0022240933223963>

445 P. J. le B. Williams. (1998). The balance of plankton respiration and photosynthesis in the open  
446 oceans. *Nature*, 394(6688), Article 6688. <https://doi.org/10.1038/27878>

447 Ryan, J. P., Ueki, I., Chao, Y., Zhang, H., Polito, P. S., & Chavez, F. P. (2006). Western Pacific  
448 modulation of large phytoplankton blooms in the central and eastern equatorial Pacific. *Journal*  
449 *of Geophysical Research: Biogeosciences*, 111(G2). <https://doi.org/10.1029/2005JG000084>

450 Schut, F., Prins, R., & Gottschal, J. (1997). Oligotrophy and pelagic marine bacteria: Facts and  
451 fiction. *Aquatic Microbial Ecology*, 12, 177–202. <https://doi.org/10.3354/ame012177>

452 Timmermann, A., An, S.-I., Kug, J.-S., Jin, F.-F., Cai, W., Capotondi, A., Cobb, K. M.,  
453 Lengaigne, M., McPhaden, M. J., Stuecker, M. F., Stein, K., Wittenberg, A. T., Yun, K.-S., Bayr,  
454 T., Chen, H.-C., Chikamoto, Y., Dewitte, B., Dommenges, D., Grothe, P., ... Zhang, X. (2018).  
455 El Niño–Southern Oscillation complexity. *Nature*, 559(7715), 535–545.  
456 <https://doi.org/10.1038/s41586-018-0252-6>

457